Therapeutic effects of human umbilical cord mesenchymal stem cell-derived extracellular vesicles on ovarian functions through the PI3K/Akt cascade in mice with premature ovarian failure

Nan Li, Xue Fan, Lihong Liu, Yanbing Liu

Department of Gynecological Ward, The Third Affiliated Hospital, Jinzhou Medical University, Jinzhou, Liaoning Province, China

ABSTRACT

Premature ovarian failure (POF) mainly refers to ovarian dysfunction in females younger than forty. Mesenchymal stem cells (MSCs) are considered an increasingly promising therapy for POF. This study intended to uncover the therapeutic effects of human umbilical cord MSC-derived extracellular vesicles (hucMSC-EVs) on POF. hucMSCs were identified by observing morphology and examining differentiation capabilities. EVs were extracted from hucMSCs and later identified utilizing nanoparticle tracking analysis, transmission electron microscopy, and Western blotting. POF mouse models were established by injecting D-galactose (D-gal). The estrous cycles were assessed through vaginal cytology, and serum levels of follicle-stimulating hormone (FSH), luteinizing hormone (LH), anti-mullerian hormone (AMH), estradiol (E2), and progesterone (P) were measured by ELISA. The human ovarian granulosa cell line KGN was used for *in vitro* experiments. The uptake of hucMSC-EVs by KGN cells was detected. After D-gal treatment, cell proliferation and apoptosis were assessed *via* CCK-8 assay and flow cytometry. The PI3K/Akt pathway-related proteins were determined by Western blotting. Our results revealed that POF mice had prolonged estrous cycles, increased FSH and LH levels, and decreased AMH, E2, and P levels. Treatment with hucMSC-EVs partially counteracted the above changes. D-gal treatment reduced proliferation and raised apoptosis in KGN cells, while hucMSC-EV treatment annulled the changes. D-gal-treated cells exhibited downregulated p-PI3K/PI3K and p-Akt/Akt levels, while hucMSC-EVs activated the PI3K/Akt pathway. LY294002 suppressed the roles of hucMSC-EVs in promoting KGN cell proliferation and lowering apoptosis. Collectively, hucMSC-EVs facilitate proliferation and suppress apoptosis of ovarian granulosa cells by activating the PI3K/Akt pathway, thereby alleviating POF.

Key words: Premature ovarian failure; human umbilical cord mesenchymal stem cells; extracellular vesicles; PI3K/Akt; therapeutic effects; D-galactose.

Correspondence: Xue Fan, Department of Gynecological Ward, The Third Affiliated Hospital, Jinzhou Medical University, No.2, Section 5, Heping Road, Linghe District, Jinzhou City 121000, Liaoning Province, China.
Tel.-Fax: +86.0416.3999062. E-mail: XueFan0520@163.com

Contributions: NL, contribution to the study concepts and study design; XF, guarantor of integrity of the entire study, contribution to the literature research and to manuscript editing and review; LL, contribution to experimental studies and data acquisition; NL, YL, contribution to the manuscript preparation. All the authors read and approved the final version of the manuscript and agreed to be accountable for all aspects of the work.

Conflict of interest: the authors declare that they have no competing interests, and all authors confirm accuracy.

Ethics approval: all involved animal experiments were ratified by the Ethics Committee of The Third Affiliated Hospital, Jinzhou Medical University (JZ2021023). We made considerable efforts to minimize the animal quantity and their pain.

Availability of data and materials: all the data generated or analyzed during this study are included in this published article.

Funding: this study was supported by a grant from the application of PTEN gene overexpression in the experimental study of improving chemotherapy-induced premature ovarian failure (no. JYTJT20221543).

Introduction

Premature ovarian failure (POF), also known as primary or premature ovarian insufficiency (POI), is an infertility disorder in humans that affects 1-5% of women younger than 40 years.[1] The occurrence of POF is mainly attributed to dysfunctional ovarian follicles or decreased primordial follicles.[2] The nongenetic causes of POF include autoimmune diseases, viral infections, radiotherapy, or chemotherapy, while genetic causes are highly heterogeneous, including both isolated (nonsyndromic) and syndromic POF.[3] The typical symptoms of POF consist of hormonal deficits, infertility, vaginal dryness, discomfort during sexual intercourse, irregular menstruation, night sweating, and emotional problems.[4] In terms of treatments, *in vitro* activation, regenerative medicine, and hormone therapy are well-known and commonly utilized therapies for POF; however, these modalities may be accompanied by several complications.[5,6] Thereby, more effective and potent therapeutic strategies for POF are of utmost urgency and importance to restore ovarian function, thus alleviating adverse consequences.

Extracellular vesicles (EVs) are intrinsically considered to be membrane-bound vesicles released from prokaryotic and eukaryotic cells, which can potentially transport multifarious cargoes including DNA, RNA, proteins, and lipids, serving as vital vehicles of intercellular communication.[7,8] Based on the distinct biological properties, including size, biomarker, and biogenesis pathways, EVs are classified mainly into apoptotic bodies, microvesicles, and exosomes.[9] Typically, an array of cells, such as cancer cells, endothelial cells, epithelial cells, platelets, leukocytes, neurons, fibroblasts, and mesenchymal stem cells (MSCs), can secrete EVs.[10,11] Due to the self-renewal and regeneration potential,[12] stem cells are exceedingly utilized to potently treat POF, with beneficial effects on ovarian angiogenesis, structural and functional restoration, follicular activation, and hormonal level recovery.[4,13] As one of the intensively studied MSCs, human umbilical cord MSCs (hucMSCs) emerge as ideal therapeutic means due to their unique advantages such as large cell content, low cost, noninvasive collection procedures, easy extraction and expansion, low immunogenicity, high proliferation, and low infection risk, and the hucMSC-derived EVs (hucMSC-EVs) have shown therapeutic effects in cardiovascular, neurological, kidney, liver, and bone diseases, cancer, and infertility.[14] To this end, investigating the precise therapeutic roles of hucMSC-EVs in POF is imperative for clinical treatment.

Many researchers have documented the paramount importance of phosphatidylinositol 3-kinase/protein kinase B (PI3K/Akt) cascade in primordial follicle activation.[15,16] The suppressed PI3K/Akt signaling essentially prevents granulosa cell growth and induces apoptosis,[17] which also probably contributes to large-scale oocyte loss, ultimately causing POF.[18] Interestingly, *Evodiae fructus* extract alleviates 4-vinylcyclohexene diepoxide-induced ovotoxicity in ovary cells by activating the PI3K/Akt pathway, showing potential in preventing POF.[19] Therefore, we proposed a hypothesis that MSC-EVs might exert a therapeutic role in POF through the PI3K/Akt pathway. Accumulating reports reveal that D-galactose (D-gal) treatment leads to excessive formation of reactive oxygen species (ROS) and accumulation of advanced glycation endproducts (AGE) in the brain, myocardium, liver, kidney, muscle, blood vessel, and ovary of mice,[20-2], which are primary causes of ovarian aging that gradually impairs ovarian functions.[26] Because the accelerated aging process in the D-gal-induced aging model is highly similar to that occurring during aging in humans, this model is widely used to explore the mechanism of POF.[2]. Therefore, in the current study, POF mouse models were established by injecting D-gal to explore the action and mechanism of hucMSC-EVs in POF, so as to provide new insights into POF treatment and management.

Materials and Methods

Culture and identification of hucMSCs

The hucMSC line CP-CL11 provided by Procell (Wuhan, China) was cultured in Dulbecco's modified Eagle medium (DMEM) added with 10% fetal bovine serum (FBS), 100 U/mL penicillin, and 100% μg/mL streptomycin (Solarbio, Beijing, China) in a 37°C incubator with 5% CO_2.

The procedures of Oil red O staining for detection of adipogenic differentiation of hucMSCs were as follows: hucMSCs were induced for adipogenic differentiation using OriCell™ hucMSC Adipogenic Differentiation Kits (HUXUC-90031, Cyagen Biosciences, Santa Clara, CA, USA). Cells were seeded at a density of 2×10^4 cells/cm^2 in 6-well culture plates and subsequently cultured in human MSC serum-free medium. When confluence reached 100%, cells were cultured in hucMSC adipogenic differentiation medium for 21 days and then fixed with 4% neutral formaldehyde for 30 min at room temperature. Cells were stained with 0.5% Oil red O (Sigma-Aldrich, Merck KGaA, Darmstadt, Germany) for 40 min at room temperature. Cells were rinsed twice with phosphate-buffered saline (PBS), stained with Harris hematoxylin (Surgipath, Bretton, UK) for 45 s, and washed with tap water (turned blue) for 1 to 3 min, followed by washing with distilled water. The peripheral water was aspirated using paper towels, and the slides were mounted using glycerin gelatin. Cells were observed under a light microscope (Olympus, Tokyo, Japan) at a magnification of 200× and images were captured.

The steps of Alizarin red staining for detection of osteogenic differentiation of hucMSCs were as follows: osteogenic differentiation was induced in hucMSCs by OriCell™ hucMSC Osteogenic Differentiation Kits (HUXUC-90021, Cyagen Biosciences). Cells were seeded at a density of 1×10^4 cells/cm^2 in 24-well culture plates and subsequently cultured in human MSC serum-free medium. When confluence reached 80-90%, cells were cultured in hucMSC osteogenic differentiation medium for 21 days and subsequently fixed for 30 min with 4% neutral formaldehyde at room temperature. Cells were subsequently washed with PBS for 2 min, stained with 10% Alizarin red (Yeasen, Shanghai, China) for 10 min at room temperature, and rinsed thrice with PBS. The fluid was discarded, and the slides were mounted with neutral gum. Cells were observed under a light microscope (200×, Olympus) and images were obtained.

EVs extraction and identification

The conditional medium (CM) of hucMSCs was centrifuged at 2,000×g for 30 min at 4°C to remove cell debris, and next the supernatant was ultracentrifuged (Optima XPN-100, Beckman Coulter, Chaska, MN, USA) at 100,000×g for 2 h at 4°C. The supernatant was discarded, and the sediments were resuspended in PBS and ultracentrifuged again at 100,000×g for 2 h. The concentrated hucMSC-EVs were then resuspended in PBS.[28] The number of hucMSC-EVs was determined by measuring total protein content using the Bradford method, and the diluted bovine serum albumin gradient was employed to plot standard curves.[29,30] The morphology of EVs was observed under a transmission electron microscope (TEM; HT7800, Hitachi, Japan), and the particle size was measured with a nanoparticle tracking analyzer (NTA; Malvern Instruments, Malvern, UK). GW4869 is widely used to inhibit the secretion of EVs,[31,32] and therefore we used it as a negative control for EVs in this study. hucMSCs were cultured in EV-free FBS medium supplemented with GW4869 (20 μg/mL CM; Sigma-Aldrich) for 48 h and later the CM was taken and used as the control. The expression levels of EV surface markers Calnexin

(ab22595, Abcam, Cambridge, UK), CD9 (ab236630, Abcam), CD81 (ab219209, Abcam), and CD63 (ab134045, Abcam) were determined using Western blotting.

Experimental animals

C57BL/6 female mice aged 6-8 weeks were acquired from SIMR Biotechnology (License No. SCXK [Shanghai] 2022-0004, Shanghai, China). Mice were housed in a pathogen-free animal facility under 12-h dark/light cycles, with *ad libitum* access to food and water. The D-gal-induced POF model is used as a model of ovarian aging in mice.[33,34] Firstly, mice were randomized to 4 groups (6 mice per group): control group, POF group, POF + GW4869 group, and POF + EVs group. Mice in the POF, POF + GW4869, and POF + EVs groups were subcutaneously injected with 600 mg/kg/day D-gal ($C_6H_{12}O_6$, Sigma-Aldrich) once a day for 42 days. The control mice were only injected with an equal amount of normal saline. Mice in the POF + EVs/GW4869 groups were injected with D-gal and next injected with 0.2 mL PBS containing 1×10^8/mL hucMSC-EVs or GW4869 through tail veins every 2 days. One week after the last injection, mice were euthanized with 800 mg/kg pentobarbital sodium and the peripheral blood of mice was collected.

Estrous cycles

Estrous cycles were monitored by vaginal smears for 12 consecutive days following D-gal treatment to assess the estrous cycle stages in mice. Vaginal lavage samples were diluted with sodium chloride injection at appropriate concentrations. Afterward, cells were evenly distributed over clean slides utilizing a centrifugal smear dyeing machine (Cytopro 7, 621, Norwalk, CA, USA), fixed in absolute ethanol for 10 s, and then stained with Wright-Giemsa Stain (Baso Diagnostics, Zhuhai, China). Vaginal cells were analyzed under a light microscope based on morphological criteria. The length of each cycle was evaluated as the time span between two consecutive estrous cycles.

ELISA

The peripheral blood samples were allowed to clot for 60 min and later centrifuged at 1,000×g for 15 min to collect the serum, followed by preservation at -80°C. The levels of follicle-stimulating hormone (FSH), luteinizing hormone (LH), anti-Mullerian hormone (AMH), estradiol (E2), and progesterone (P) were determined using ELISA kits.

Culture of ovarian granulosa cells

The ovarian granulosa cells (KGN cell line; Procell) were cultured in DMEM (Sigma-Aldrich) added with 10% FBS (Sigma-Aldrich) and 1% antibiotic/antifungal solution (Invitrogen, Carlsbad, CA, USA). KGN cells in the 2nd generation were put in 6-well plates at a density of 1×10^5 cells/well. After 24 h, the original medium was discarded, and cells were only treated with DMEM/F12 medium (Invitrogen) for 24 h to starve the cells. Thereafter, KGN cells were assigned into 6 groups: blank (without treatment), D-gal (medium was added with 100 nM D-gal[35]), D-gal + EVs (medium was supplemented with 100 nM D-gal and hucMSC-EVs at a density of 1×10^8 particles/mL), D-gal + GW4869 (the CM was added with 100 nM D-gal and equivalent GW4869), D-gal + EVs + LY294002 (medium was supplemented with 100 nM D-gal, an equivalent volume of hucMSC-EVs, and 50 μM PI3K/Akt inhibitor LY294002[36] purchased from Abcam), and D-gal + EVs + DMSO (medium was supplemented with 100 nM D-gal and equivalent volumes of hucMSC-EVs and dimethyl sulphoxide [DMSO]).

Labeling of EVs

The 100 μL of EV suspension was supplemented with 1 mL of dilution C-diluted PKH67 (Sigma-Aldrich) for 4 min. The reaction was subsequently terminated *via* exposure to 1 mL of 0.5% bovine serum albumin, and later the extraction kits were employed to re-extract EVs. After labeling with PKH67, under a confocal laser scanning microscope EVs appeared green. KGN cells were stained blue with 4',6-diamidino-2-phenylindole (DAPI; Sigma-Aldrich). PKH67-labeled EVs were co-cultured with KGN cells for 24 h, followed by localization. The specific steps were as follows: KGN cells were cultured in 4-well plates for 24 h and then the well was added with PKH67-labeled hucMSC-EVs, followed by incubation for 24 h at 37°C. Thereafter, cells were rinsed thrice with cold PBS and fixed with 2% paraformaldehyde for 10 min at room temperature. Next, cells were permeabilized with 0.1% Triton X-100 (Sigma-Aldrich) for 2 min, rinsed with PBS thrice, and stained with DAPI (10 μg/mL) for 5 min at room temperature. Images were then captured with a fluorescence microscope (Olympus).

CCK-8 assay

Cells were seeded in 96-well plates at a density of 2×10^4 cells/mL. After 24 h, cell viability was examined by CCK-8 assay. In brief, the corresponding volume of CCK-8 reagent was added to each well and mixed well, followed by culture for 1.5 h in an incubator containing 5% CO_2 at 37°C. The optical density (OD) value at 450 nm was then determined on a microplate reader.

Flow cytometry

Cells were put in 24-well plates at a density of 1×10^6 cells/mL. After 48-h incubation, cells were collected and resuspended. Afterward, 100 μL of cell resuspension was stained with 5 μL of 1 μg/mL Annexin V-fluorescein isothiocyanate and 5 μL of 2.5 μg/mL propidium iodide (Vazyme, Nanjing, China) for 20 min. Finally, the apoptosis rate was calculated utilizing a flow cytometer (BD Biosciences, San Jose, CA, USA). Each experiment was repeated thrice.

Western blotting

Protein was obtained through lysis of cells or EVs using radioimmunoprecipitation assay buffer (Thermo Fisher Scientific, Waltham, MA, USA). Protein concentration was measured with bicinchoninic acid kits (Sigma-Aldrich). Proteins were subjected to sodium dodecyl sulfate-polyacrylamide gel electrophoresis, followed by membrane transferring. Membranes were probed with 4 mL primary antibodies overnight at 4°C. Subsequently, membranes were rinsed thrice and later incubated with horseradish peroxidase-conjugated goat anti-rabbit secondary antibody for 2 h. The ratio of the gray value of the target protein bands to that of glyceraldehyde-3-phosphate dehydrogenase (GAPDH) reflected the relative expression of target proteins, and the relative protein expression was semi-quantitatively analyzed with image analysis software BandScan 5.0 (BioMarin, San Rafael, CA, USA). (Primary antibodies: Calnexin, 1:1000, ab22595; CD9, 1:1000, ab236630; CD81, 1:1000, ab219209; CD63, 1:1000, ab134045; PI3K, 1:1000, ab32089; p-PI3K, 1:1000, ab182651; Akt: 1:1000, ab38449; p-Akt: 1:1000, ab81283; GAPDH, 1:1000, ab9485; secondary antibody IgG: 1:2000, ab205718; all from Abcam).

Statistical analysis

Data analysis was processed using SPSS 21.0 (IBM Corp., Armonk, NY, USA) software. Measurement data were displayed as mean ± standard deviation (SD). The cell experiment was independently repeated thrice and the animal experiment was performed using 6 mice per group. The results of animal experiments were represented as scatter charts. The independent sample *t*-test

was conducted for comparisons between two groups and one-way analysis of variance (ANOVA) was implemented for comparisons among multiple groups. Tukey's multiple comparisons test was employed for the post hoc analysis. The $p<0.05$ was regarded as statistically significant.

Results

Identification of hucMSCs and EVs

To investigate the role of hucMSC-EVs, we purchased and then identified hucMSCs. Firstly, the morphology of hucMSCs was observed under a microscope, which indicated that hucMSCs grew in a monolayer mode and showed fibroblast-like characteristics (with a long-fusiform shape) (Figure 1A). Oil red O and Alizarin red stainings suggested that hucMSCs could differentiate into adipocytes or osteocytes after induction. After induction of adipogenic differentiation, a large number of long spindle-shaped or polygonal lipid droplets appeared in the cells; after induction of osteogenic differentiation, the whole cells were filled with calcium granules, the cells grew in colonies, and the central cells gradually fused, lost the typical cell structure, and formed clear calcium nodules (Figure 1B). In addition, the morphology and particle size of EVs were analyzed by TEM and NTA, which delineated that EVs appeared to be round or elliptical, with a complete bilayer vesicle structure and a diameter of 30-200 nm, which were in line with the general characteristics of EVs (Figure 1 C,D). Finally, Western blotting discovered that EV markers CD9, CD81, and CD63 were positively expressed, while the negative control Calnexin, an endoplasmic reticulum marker, was not expressed (Figure 1E). The aforementioned results elicited the successful isolation of hucMSC-EVs.

hucMSC-EVs ameliorated POF in mice

The mouse models of POF were induced using D-gal to validate whether hucMSC-EVs can affect POF. The observation through vaginal smears unveiled that D-gal-induced POF mice exhibited prolonged estrous cycles (Figure 2A). ELISA revealed that POF mice had increased FSH and LH levels, but decreased AMH, E2, and P levels in the serum (Figure 2B, all $p<0.01$). However, treatment with hucMSC-EVs partially annulled the above changes in estrous cycles and levels of serum hormones FSH, LH, AMH, E2, and P (Figure 2A-B, all $p<0.01$). Taken together, hucMSC-EVs could mitigate POF in mice to a significant extent.

hucMSC-EVs facilitated proliferation and prevented apoptosis of ovarian granulosa cells

To further explore whether hucMSC-EVs alleviate POF by mediating ovarian granulosa cells, the purchased ovarian granulosa cell line KGN was co-cultured with PKH67-labeled hucMSC-EVs for 24 h. The uptake assay of hucMSC-EVs by KGN cells revealed that an enormous number of hucMSC-EVs entered KGN cells and distributed around the nucleus (Figure 3A).

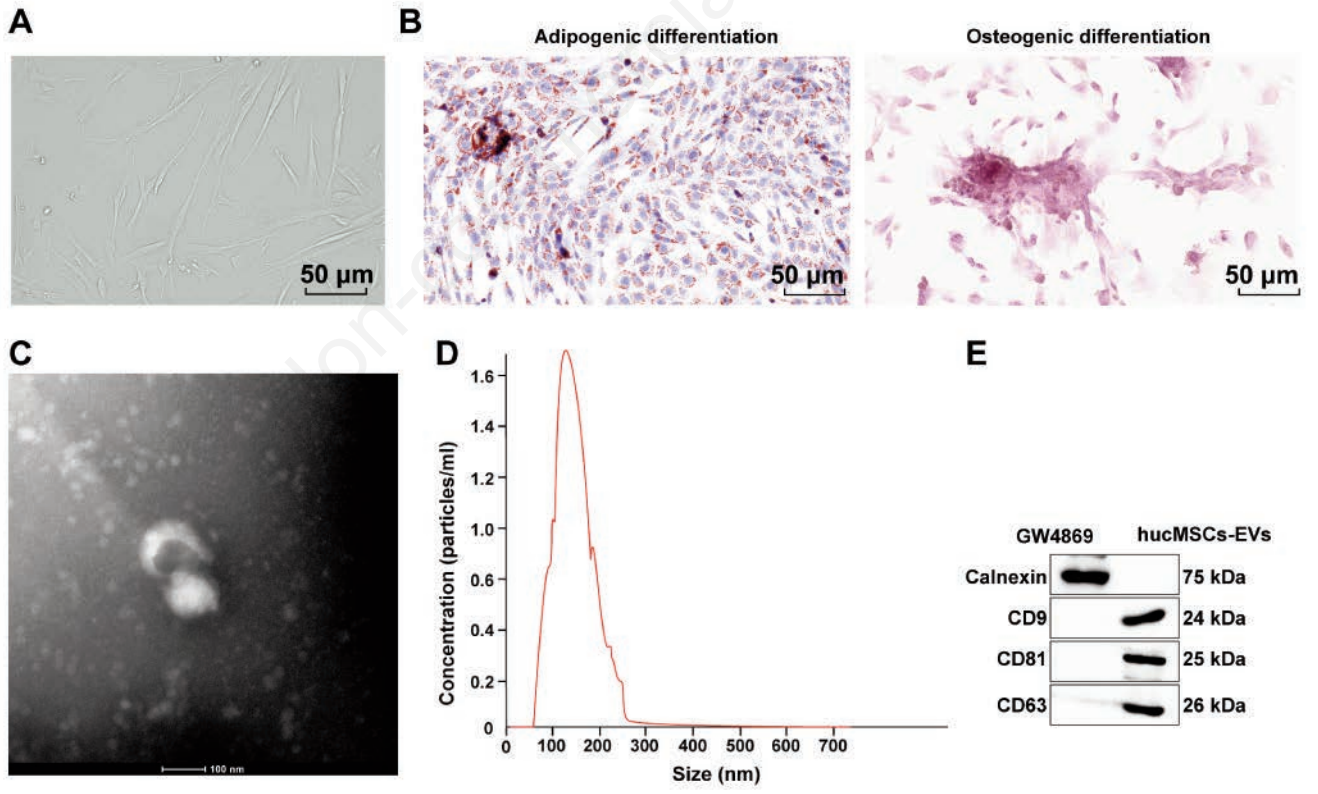

Figure 1. Identification of hucMSCs and EVs. **A**) Cell morphology of hucMSCs observed under an inverted microscope. **B**) Adipogenic and osteogenic differentiation abilities of hucMSCs assessed by oil red O and Alizarin red stainings, respectively. **C**) Ultrastructure of EVs observed through TEM; **D**) Diameter distribution and concentration of EVs detected by NTA. **E**) Expression of EV marker proteins CD9, CD81, CD63, and endoplasmic reticulum marker Calnexin determined by Western blotting. Cell experiment was independently repeated thrice.

Subsequently, CCK-8 assay and flow cytometry delineated that D-gal-treated KGN cells showed lowered proliferation and raised apoptosis, while further hucMSC-EVs treatment to some extent ameliorated the decrease in proliferation and increase in apoptosis (Figure 3 B,C, all $p<0.01$). In summary, hucMSC-EVs potentiated proliferation and restrained apoptosis of ovarian granulosa cells.

hucMSC-EVs promoted functional recovery of ovarian granulosa cells through the PI3K/Akt pathway

Mounting evidence reveals the protection role of the PI3K/Akt pathway activation in ovarian aging,[37,38] and hence we proposed that hucMSC-EVs promote the functional restoration of ovarian granulosa cells by activating the PI3K/Akt pathway. The marker proteins of the PI3K/Akt pathway were determined by Western blotting, which unraveled that p-PI3K/PI3K and p-Akt/Akt in KGN cells were prominently downregulated after D-gal treatment; the downregulation of p-PI3K/PI3K and p-Akt/Akt was partially annulled upon hucMSC-EV treatment; further treatment with LY294002, a PI3K pathway inhibitor, weakened the effect of hucMSC-EVs on activating the PI3K/Akt pathway (Figure 4A, all $p<0.01$). Meanwhile, CCK-8 and flow cytometry demonstrated that LY294002 suppressed the roles of hucMSC-EVs in promoting KGN cell proliferation and lowering apoptosis rate (Figure 4 B,C, all $p<0.01$). Briefly, hucMSC-EVs promoted proliferation and repressed apoptosis of ovarian granulosa cells by activating the PI3K/Akt pathway, thereby improving POF.

Discussion

POF is commonly construed as a syndrome comprising sex steroid deficiency, gonadotropin elevation, and amenorrhea in women under the age of 40, resulting in infertility and considerable psychological stress.[39] EVs are currently gaining a great deal of attention from researchers for their specific release mechanisms, participation in cell-to-cell signaling, and utility as biomarkers or therapeutic targets for diseases.[40] Of note, MSC-EVs confer therapeutic roles in diverse female reproductive disorders, such as POI, polycystic ovary syndrome, and intrauterine adhesion.[41,42] Currently, studies on the treatment of POF are mostly based on *in vitro* cell experiments and *in vivo* animal models.[36,43-45] Prior clinical study has investigated the therapeutic use of intramuscular injection of MSCs for the treatment of uterine niche after cesarean delivery.[46] However, research on the therapeutic effect of hucMSC-EVs on POF at the clinical level is indeed rare. This study explored the therapeutic mechanism of hucMSC-EVs in POF and highlighted that hucMSC-EVs restored ovarian function *via* the PI3K/Akt cascade in POF mice.

As a widely used model of aging in mice, the D-gal-induced

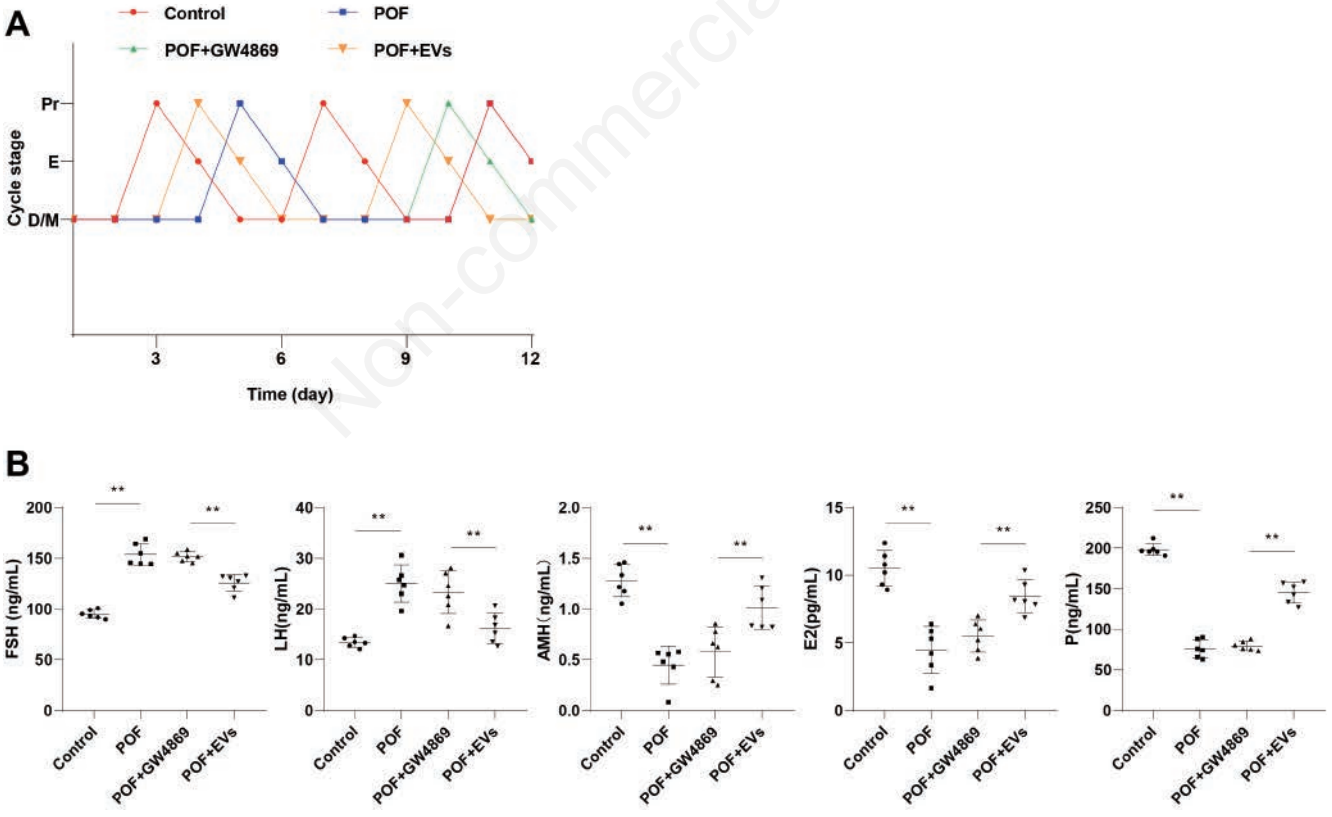

Figure 2. hucMSC-EVs ameliorated POF in mice. POF mouse models were induced using D-gal and then treated with hucMSC-EVs, with GW4869 as the control. **A**) Vaginal cytology assessed estrous cycles in pro-estrus (Pr), estrus (E), metestrus (M), and diestrus (D) over the course of 12 consecutive days. **B**) ELISA determined the serum levels of FSH, LH, AMH, E2, and P; n=6. Analysis of measurement data was processed using one-way ANOVA, followed by Tukey's test; **p<0.01.

POF model is generally employed to explore the potential mechanisms of ovarian aging, as accelerated aging extremely resembles the observation in humans.[47] Therefore, in our experiments, POF mouse models were also induced by subcutaneously injecting D-gal. It is broadly well-known that estrous cycles and sex hormone secretion are commonly used for the evaluation of ovarian function.[48] POF is typically characterized by low AMH and gonadal hormones (inhibins and estrogens), high gonadotropins including FSH and LH (hypergonadotropic amenorrhea), and LH in conjunction with FSH can modulate the production of steroid sex hormones E2 and P through theca cells surrounding growing follicles in the ovary.[49,50] Not surprisingly, our results unearthed that POF mice presented prolonged estrous cycles, raised FSH and LH levels, and diminished AMH, E2, and p-levels in the serum. GW4869 (a cell-permeable symmetrical dihydroimidazolamide compound), is a potent, specific, and non-competitive inhibitor of membrane-neutral sphingomyelinase,[51,52] which can efficiently inhibit the secretion of EVs.[31,32] Therefore, GW4869 was used as a negative control for EVs in this study. In subsequent experiments, hucMSC-EV treatment shortened estrous cycles and partially reversed the above trends in serum hormones. Consistently, embryonic stem cell-secreted EVs can restore E2, AMH, and FSH to normal levels, reduce atresia, and elevate the number of normal follicles.[36] It is noteworthy that hucMSCs have the advantages of easy extraction and expansion, cost-effectiveness, non-invasive collection process, high cell content, and a small risk of infection, making them highly suitable for therapeutic applications.[14,53,54] As one of the major extracellular signaling pathways, EVs are associated with a variety of diseases and are involved in diverse physiological processes.[55,56] Compared to other EVs, hucMSC-EVs have a greater potential for treatment due to their low immunogenicity, toxicity, invasiveness, and cost-effectiveness.[14] Importantly, hucMSC-EVs can promote functional recovery in mice with spinal cord injury by alleviating inflammatory responses.[57] hucMSC-EVs carrying miR-29a evidently improve ovarian function by targeting HBP1 and activating the Wnt/β-catenin pathway.[58] In the above studies, the use of hucMSC-EVs shows no toxicities or off-target effects in mice. Mounting studies have revealed the alleviation roles of hucMSCs transplantation in POF animals, as supported by the recovery in ovarian function and hormone levels, improvement in sexual cycle disorder, and an increase in ovarian volume, antral follicle number, and ovarian angiogenesis.[59,6]. The above findings elucidated that hucMSC-EVs certainly have a definitive alleviating effect on POF by normalizing estrous cycles and hormone levels.

As critical somatic components of the ovary, granulosa cells are necessitated for follicle development by supporting oocyte development and producing disparate growth factors and sex steroids.[61] In mechanism, granulosa cell apoptosis is considered a vital contributor to POF; conversely, inhibition of apoptosis can mitigate POF in animal models.[62] Owing to the imperative proper-

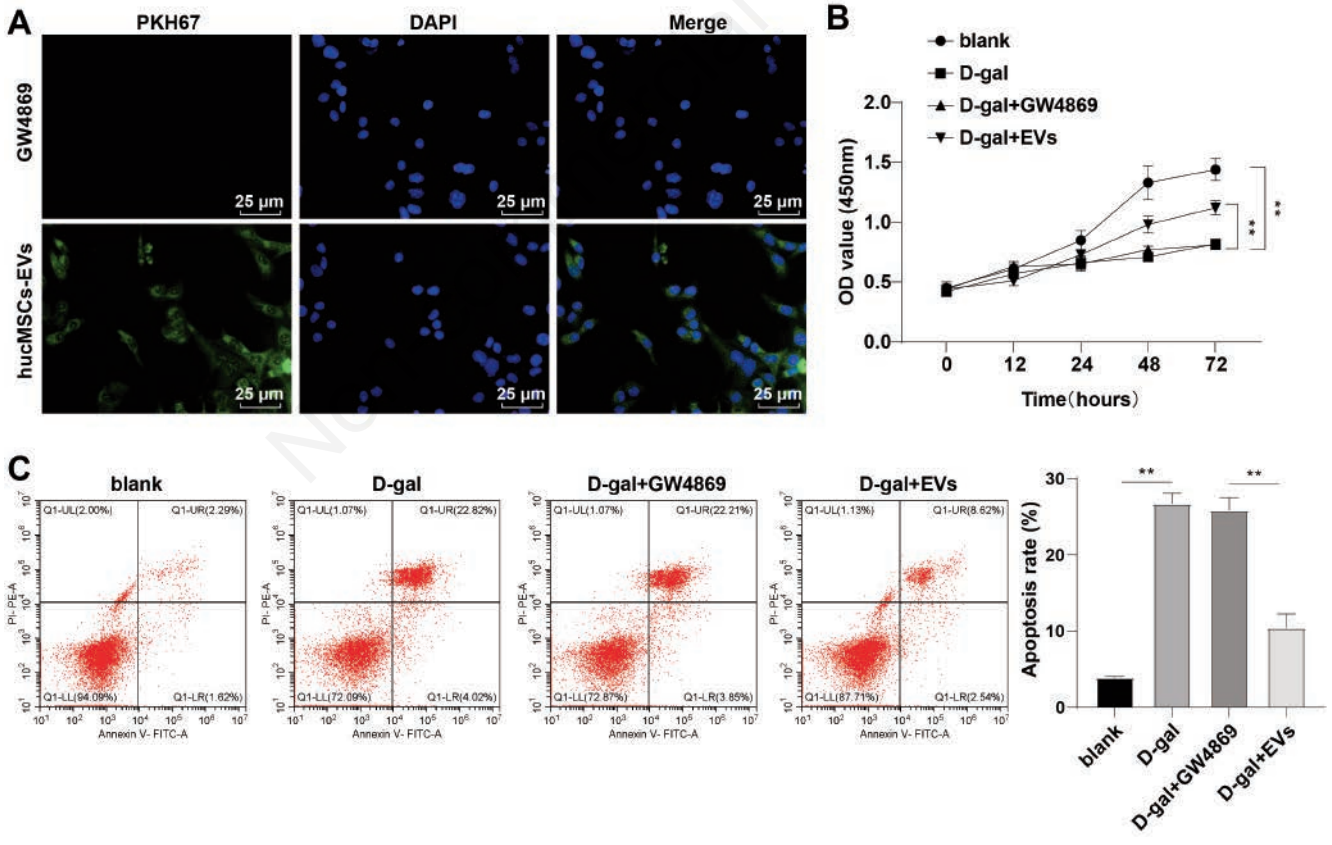

Figure 3. hucMSC-EVs facilitated proliferation and prevented apoptosis of ovarian granulosa cells. The purchased ovarian granulosa cell line KGN was treated with D-gal to induce senescence. **A**) Immunofluorescence detected the entry of PKH67-labeled hucMSC-EVs into KGN cells. **B**) CCK-8 assay assessed cell proliferation. **C**) Flow cytometry assessed cell apoptosis. Cell experimentation was independently repeated thrice. Measurement data were exhibited as mean ±SD. Data analysis was conducted using one-way ANOVA, followed by Tukey's test; **p<0.01.

ty of ovarian granulosa cells in POF, we conducted *in vitro* experiments by using the purchased ovarian granulosa cell line KGN. Our results evinced that D-gal-treated KGN cells exhibited decreased proliferation and elevated apoptosis. It is worth noting that hucMSC-derived exosomes can potentiate ovarian granulosa cell proliferation and impede apoptosis.[44,63] In agreement with the preceding research, our findings ascertained that hucMSC-EVs ameliorated the D-gal-induced injury on KGN cells.

Intrinsically, E2, a hormone with high biological activity in women, not only shows a considerable role in regulating gene transcription but also activates the PI3K pathway together with estrogen receptors on the cell membrane.[64] Notably, POI patients have successful pregnancies after grafting the small ovarian fragments that are exposed to PI3K/Akt activators, primarily due to the critical property of the PI3K/Akt/mTOR cascade in follicular recruitment and growth.[15] Moreover, several therapies for POF, such as resveratrol and acupuncture decrease granulosa cell apoptosis in POF rats through the restoration of the PI3K/Akt pathway.[64,65] Preceding research has given rise to the necessity of exploring the primary roles of the PI3K/Akt pathway in KGN cell growth. We noted that p-PI3K/PI3K and p-Akt/Akt were downregulated in D-gal-treated KGN cells but upregulated after the addition of hucMSC-EVs. Consistently, hucMSC-derived microvesicles can upregulate the AKT and p-AKT levels in the ovaries of POI mice.[6] In addition, a PI3K pathway inhibitor, LY294002 impeded the effects of hucMSC-EVs on enhancing KGN cell proliferation and weakening apoptosis. In response to the PI3K/Akt pathway stimulators, mTORC1 in granulosa cells is activated, and subsequently, granulosa cells start to cuboidalize, proliferate, and exclude SMADs proteins.[67] Compelling evidence suggests a similar mechanism of embryonic stem cell-derived EVs in affecting granulosa cells *via* promotion in the PI3K/Akt pathway.[36] Collectively, hucMSC-EVs potentiated proliferation and restrained apoptosis in KGN cells by activating the PI3K/Akt pathway.

In conclusion, the present study highlighted that hucMSC-EVs shortened the estrous cycles of POF mice, facilitated KGN cell proliferation, and repressed apoptosis *via* activation of the PI3K/Akt pathway, thereby ameliorating POF. On the downside, we only investigated the regulation of hucMSC-EVs on serum sexual hormones in POF mice and ovarian granulosa cells, lacking investigation of animal tissues. The utilization of artificial ovary as a promising alternative to restore fertility has been investigated by many researchers around the world.[68,69] As a human transplantable artificial ovary, it should allow follicular survival and proliferation, facilitate the formation of blood vessels and stroma *in vivo*, and be safe for the human body.[70] Future experiments shall be designed to deeply explore the effects of hucMSC-EVs on POF using animal tissues or pathological tissues from clinical patients and their precise regulatory mechanisms in the PI3K/Akt cascade. Additionally, more *in vivo* experiments should be performed to find appropriate transplantable artificial ovarian scaffolds to provide more information for clinical application.

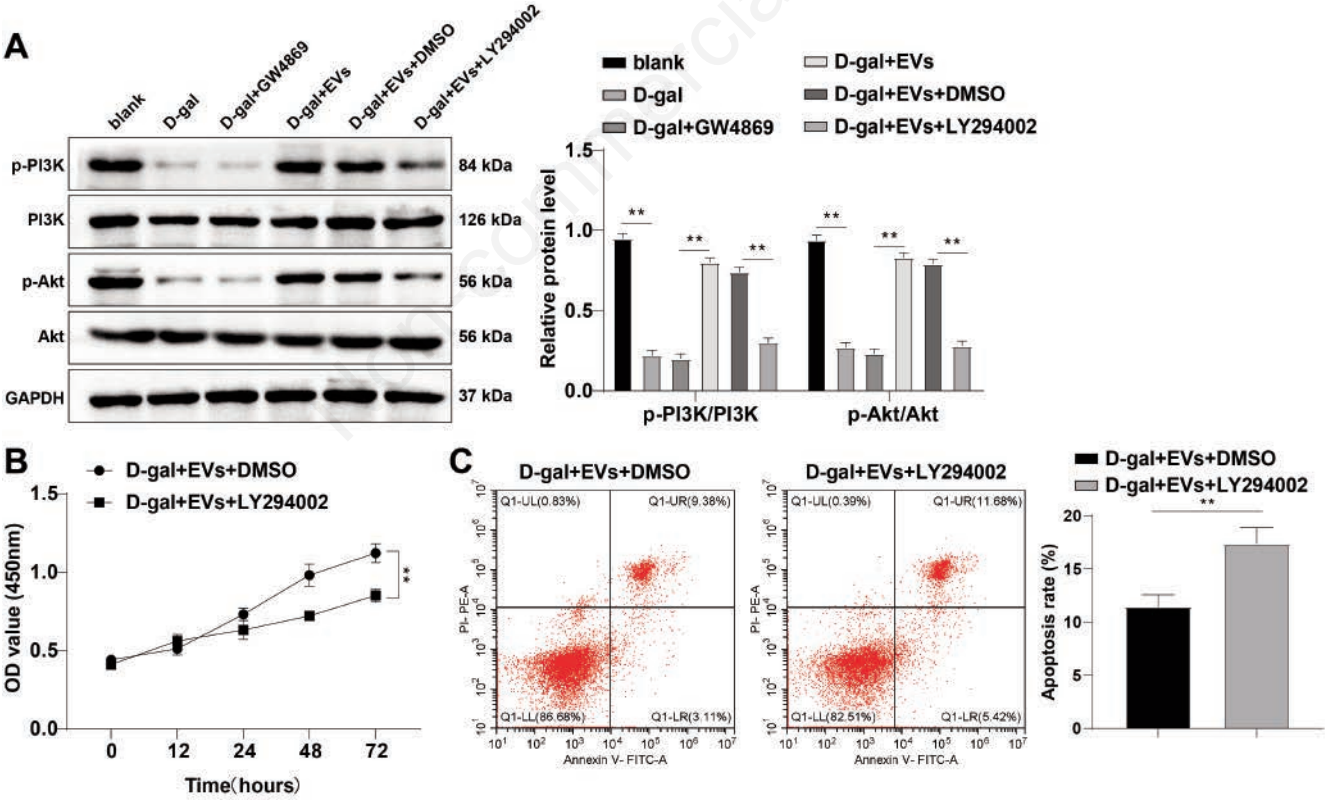

Figure 4. hucMSC-EVs promoted functional recovery of ovarian granulosa cells through the PI3K/Akt pathway. The PI3K/Akt pathway was blocked using LY294002, a PI3K pathway inhibitor, with DMSO as the control. **A**) Western blotting determined the protein levels of p-PI3K/PI3K and p-Akt/Akt. **B**) CCK-8 assay evaluated cell proliferation. **C**) Flow cytometry evaluated cell apoptosis. Cell experimentation was independently conducted thrice. Measurement data were shown as mean ±SD. One-way ANOVA was employed for data analysis in panel A, followed by Tukey's test. An independent sample t-test was used for data analysis in panels B/C; **p<0.01.

References

1. Goswami D, Conway GS. Premature ovarian failure. Hum Reprod Update 2005;11:391-410.
2. Sassarini J, Lumsden MA, Critchley HO. Sex hormone replacement in ovarian failure - new treatment concepts. Best Pract Res Clin Endocrinol Metab 2015;29:105-14.
3. Pierce SB, Gersak K, Michaelson-Cohen R, Walsh T, Lee MK, Malach D, et al. Mutations in LARS2, encoding mitochondrial leucyl-tRNA synthetase, lead to premature ovarian failure and hearing loss in Perrault syndrome. Am J Hum Genet 2013;92:614-20.
4. Wang MY, Wang YX, Li-Ling J, Xie HQ. Adult stem cell therapy for premature ovarian failure: from bench to bedside. Tissue Eng Part B Rev 2022;28:63-78.
5. European Society for Human Reproduction and Embryology (ESHRE) Guideline Group on POI, Webber L, Davies M, Anderson R, Bartlett J, et al. ESHRE Guideline: management of women with premature ovarian insufficiency. Hum Reprod 2016;31:926-37.
6. Ghahremani-Nasab M, Ghanbari E, Jahanbani Y, Mehdizadeh A, Yousefi M. Premature ovarian failure and tissue engineering. J Cell Physiol 2020;235:4217-26.
7. Leidal AM, Debnath J. Unraveling the mechanisms that specify molecules for secretion in extracellular vesicles. Methods 2020;177:15-26.
8. Sil S, Dagur RS, Liao K, Peeples ES, Hu G, Periyasamy P, et al. Strategies for the use of extracellular vesicles for the delivery of therapeutics. J Neuroimmune Pharmacol 2020; 15:422-42.
9. Thakur A, Ke X, Chen YW, Motallebnejad P, Zhang K, Lian Q, et al. The mini player with diverse functions: extracellular vesicles in cell biology, disease, and therapeutics. Protein Cell 2022;13:631-54.
10. Gao J, Dong X, Wang Z. Generation, purification and engineering of extracellular vesicles and their biomedical applications. Methods 2020;177:114-25.
11. Raposo G, Stoorvogel W. Extracellular vesicles: exosomes, microvesicles, and friends. J Cell Biol 2013;200:373-83.
12. Regmi S, Pathak S, Kim JO, Yong CS, Jeong JH. Mesenchymal stem cell therapy for the treatment of inflammatory diseases: Challenges, opportunities, and future perspectives. Eur J Cell Biol 2019;98:151041.
13. Zhang C. The roles of different stem cells in premature ovarian failure. Curr Stem Cell Res Ther 2020;15:473-81.
14. Abbaszadeh H, Ghorbani F, Derakhshani M, Movassaghpour A, Yousefi M. Human umbilical cord mesenchymal stem cell-derived extracellular vesicles: A novel therapeutic paradigm. J Cell Physiol 2020;235:706-17.
15. Grosbois J, Demeestere I. Dynamics of PI3K and Hippo signaling pathways during in vitro human follicle activation. Hum Reprod 2018;33:1705-14.
16. Kawamura K, Kawamura N, Hsueh AJ. Activation of dormant follicles: a new treatment for premature ovarian failure? Curr Opin Obstet Gynecol 2016;28:217-22.
17. Han Y, Yao R, Yang Z, Li S, Meng W, Zhang Y, et al. Interleukin-4 activates the PI3K/AKT signaling to promote apoptosis and inhibit the proliferation of granulosa cells. Exp Cell Res 2022;412:113002.
18. Liang QX, Wang ZB, Lin F, Zhang CH, Sun HM, Zhou L, et al. Ablation of beta subunit of protein kinase CK2 in mouse oocytes causes follicle atresia and premature ovarian failure. Cell Death Dis 2018;9:508.
19. Nam EY, Kim SA, Kim H, Kim SH, Han JH, Lee JH, et al. Akt activation by Evodiae fructus extract protects ovary against 4-vinylcyclohexene diepoxide-induced ovotoxicity. J Ethnopharmacol 2016;194:733-9.
20. Simm A, Casselmann C, Schubert A, Hofmann S, Reimann A, Silber RE. Age associated changes of AGE-receptor expression: RAGE upregulation is associated with human heart dysfunction. Exp Gerontol 2004;39:407-13.
21. Schinzel R, Munch G, Heidland A, Sebekova K. Advanced glycation end products in end-stage renal disease and their removal. Nephron 2001;87:295-303.
22. Nerlich AG, Schleicher ED. N(epsilon)-(carboxymethyl)lysine in atherosclerotic vascular lesions as a marker for local oxidative stress. Atherosclerosis 1999;144:41-7.
23. Kimura T, Takamatsu J, Ikeda K, Kondo A, Miyakawa T, Horiuchi S. Accumulation of advanced glycation end products of the Maillard reaction with age in human hippocampal neurons. Neurosci Lett 1996;208:53-6.
24. Hyogo H, Yamagishi S. Advanced glycation end products (AGEs) and their involvement in liver disease. Curr Pharm Des 2008;14:969-72.
25. Haus JM, Carrithers JA, Trappe SW, Trappe TA. Collagen, cross-linking, and advanced glycation end products in aging human skeletal muscle. J Appl Physiol (1985) 2007; 103:2068-76.
26. Bandyopadhyay S, Chakrabarti J, Banerjee S, Pal AK, Goswami SK, Chakravarty BN, et al. Galactose toxicity in the rat as a model for premature ovarian failure: an experimental approach readdressed. Hum Reprod 2003;18:2031-8.
27. Liang X, Yan Z, Ma W, Qian Y, Zou X, Cui Y, et al. Peroxiredoxin 4 protects against ovarian ageing by ameliorating D-galactose-induced oxidative damage in mice. Cell Death Dis 2020;11:1053.
28. Wang L, Gu Z, Zhao X, Yang N, Wang F, Deng A, et al. Extracellular vesicles released from human umbilical cord-derived mesenchymal stromal cells prevent life-threatening acute graft-versus-host disease in a mouse model of allogeneic hematopoietic stem cell transplantation. Stem Cells Dev 2016;25:1874-83.
29. Brill A, Dashevsky O, Rivo J, Gozal Y, Varon D. Platelet-derived microparticles induce angiogenesis and stimulate post-ischemic revascularization. Cardiovasc Res 2005;67: 30-8.
30. Collino F, Deregibus MC, Bruno S, Sterpone L, Aghemo G, Viltono L, et al. Microvesicles derived from adult human bone marrow and tissue specific mesenchymal stem cells shuttle selected pattern of miRNAs. PLoS One 2010; 5:e11803.
31. Wang G, Xie L, Li B, Sang W, Yan J, Li J, et al. A nanounit strategy reverses immune suppression of exosomal PD-L1 and is associated with enhanced ferroptosis. Nat Commun 2021;12:5733.
32. Luberto C, Hassler DF, Signorelli P, Okamoto Y, Sawai H, Boros E, et al. Inhibition of tumor necrosis factor-induced cell death in MCF7 by a novel inhibitor of neutral sphingomyelinase. J Biol Chem 2002;277:41128-39.
33. Song X, Bao M, Li D, Li YM. Advanced glycation in D-galactose induced mouse aging model. Mech Ageing Dev 1999;108:239-51.
34. Semba RD, Nicklett EJ, Ferrucci L. Does accumulation of advanced glycation end products contribute to the aging phenotype? J Gerontol A Biol Sci Med Sci 2010;65:963-75.
35. Banerjee S, Chakraborty P, Saha P, Bandyopadhyay SA, Banerjee S, Kabir SN. Ovotoxic effects of galactose involve attenuation of follicle-stimulating hormone bioactivity and up-regulation of granulosa cell p53 expression. PLoS One

2012;7:e30709.
36. Liu M, Qiu Y, Xue Z, Wu R, Li J, Niu X, et al. Small extracellular vesicles derived from embryonic stem cells restore ovarian function of premature ovarian failure through PI3K/AKT signaling pathway. Stem Cell Res Ther 2020; 11:3.
37. Ding C, Zou Q, Wu Y, Lu J, Qian C, Li H, et al. EGF released from human placental mesenchymal stem cells improves premature ovarian insufficiency via NRF2/HO-1 activation. Aging (Albany NY) 2020;12:2992-3009.
38. Yao J, Ma Y, Zhou S, Bao T, Mi Y, Zeng W, et al. Metformin prevents follicular atresia in aging laying chickens through activation of PI3K/AKT and calcium signaling pathways. Oxid Med Cell Longev 2020;2020:3648040.
39. Dragojevic-Dikic S, Marisavljevic D, Mitrovic A, Dikic S, Jovanovic T, Jankovic-Raznatovic S. An immunological insight into premature ovarian failure (POF). Autoimmun Rev 2010;9:771-4.
40. Witwer KW, Buzas EI, Bemis LT, Bora A, Lasser C, Lotvall J, et al. Standardization of sample collection, isolation and analysis methods in extracellular vesicle research. J Extracell Vesicles 2013;2:20360.
41. Liao Z, Liu C, Wang L, Sui C, Zhang H. Therapeutic role of mesenchymal stem cell-derived extracellular vesicles in female reproductive diseases. Front Endocrinol (Lausanne) 2021;12:665645.
42. Rezaie J, Nejati V, Mahmoodi M, Ahmadi M. Mesenchymal stem cells derived extracellular vesicles: A promising nanomedicine for drug delivery system. Biochem Pharmacol 2022;203:115167.
43. Sun B, Ma Y, Wang F, Hu L, Sun Y. miR-644-5p carried by bone mesenchymal stem cell-derived exosomes targets regulation of p53 to inhibit ovarian granulosa cell apoptosis. Stem Cell Res Ther 2019;10:360.
44. Li Z, Zhang M, Zheng J, Tian Y, Zhang H, Tan Y, et al. Human umbilical cord mesenchymal stem cell-derived exosomes improve ovarian function and proliferation of premature ovarian insufficiency by regulating the hippo signaling pathway. Front Endocrinol (Lausanne) 2021;12:711902.
45. Ding C, Zhu L, Shen H, Lu J, Zou Q, Huang C, et al. Exosomal miRNA-17-5p derived from human umbilical cord mesenchymal stem cells improves ovarian function in premature ovarian insufficiency by regulating SIRT7. Stem Cells 2020;38:1137-48.
46. Fan D, Wu S, Ye S, Wang W, Guo X, Liu Z. Umbilical cord mesenchyme stem cell local intramuscular injection for treatment of uterine niche: Protocol for a prospective, randomized, double-blinded, placebo-controlled clinical trial. Medicine (Baltimore) 2017;96:e8480.
47. Yan Z, Dai Y, Fu H, Zheng Y, Bao D, Yin Y, et al. Curcumin exerts a protective effect against premature ovarian failure in mice. J Mol Endocrinol 2018;60:261-71.
48. He L, Ling L, Wei T, Wang Y, Xiong Z. Ginsenoside Rg1 improves fertility and reduces ovarian pathological damages in premature ovarian failure model of mice. Exp Biol Med (Maywood) 2017;242:683-91.
49. Cordts EB, Christofolini DM, Dos Santos AA, Bianco B, Barbosa CP. Genetic aspects of premature ovarian failure: a literature review. Arch Gynecol Obstet 2011;283:635-43.
50. Sha C, Chen L, Lin L, Li T, Wei H, Yang M, et al. TRDMT1 participates in the DNA damage repair of granulosa cells in premature ovarian failure. Aging (Albany NY) 2021;13: 15193-213.
51. Shamseddine AA, Airola MV, Hannun YA. Roles and regulation of neutral sphingomyelinase-2 in cellular and pathological processes. Adv Biol Regul 2015;57:24-41.
52. Catalano M, O'Driscoll L. Inhibiting extracellular vesicles formation and release: a review of EV inhibitors. J Extracell Vesicles 2020;9:1703244.
53. Zhou H, Shen X, Yan C, Xiong W, Ma Z, Tan Z, et al. Extracellular vesicles derived from human umbilical cord mesenchymal stem cells alleviate osteoarthritis of the knee in mice model by interacting with METTL3 to reduce m6A of NLRP3 in macrophage. Stem Cell Res Ther 2022;13:322.
54. Yin S, Ji C, Wu P, Jin C, Qian H. Human umbilical cord mesenchymal stem cells and exosomes: bioactive ways of tissue injury repair. Am J Transl Res 2019;11:1230-40.
55. Zhu Z, Zhang Y, Zhang Y, Zhang H, Liu W, Zhang N, et al. Exosomes derived from human umbilical cord mesenchymal stem cells accelerate growth of VK2 vaginal epithelial cells through MicroRNAs in vitro. Hum Reprod 2019;34:248-60.
56. Valadi H, Ekstrom K, Bossios A, Sjostrand M, Lee JJ, Lotvall JO. Exosome-mediated transfer of mRNAs and microRNAs is a novel mechanism of genetic exchange between cells. Nat Cell Biol 2007;9:654-9.
57. Sun G, Li G, Li D, Huang W, Zhang R, Zhang H, et al. hucMSC derived exosomes promote functional recovery in spinal cord injury mice via attenuating inflammation. Mater Sci Eng C Mater Biol Appl 2018;89:194-204.
58. Gao T, Cao Y, Hu M, Du Y. Human umbilical cord mesenchymal stem cell-derived extracellular vesicles carrying MicroRNA-29a improves ovarian function of mice with primary ovarian insufficiency by targeting HMG-Box transcription factor/Wnt/beta-catenin signaling. Dis Markers 2022;2022:5045873.
59. Yang Y, Lei L, Wang S, Sheng X, Yan G, Xu L, et al. Transplantation of umbilical cord-derived mesenchymal stem cells on a collagen scaffold improves ovarian function in a premature ovarian failure model of mice. In Vitro Cell Dev Biol Anim 2019;55:302-11.
60. Zhang X, Zhang L, Li Y, Yin Z, Feng Y, Ji Y. Human umbilical cord mesenchymal stem cells (hUCMSCs) promotes the recovery of ovarian function in a rat model of premature ovarian failure (POF). Gynecol Endocrinol 2021;37:353-7.
61. Tu J, Cheung AH, Chan CL, Chan WY. The role of microRNAs in ovarian granulosa cells in health and disease. Front Endocrinol (Lausanne) 2019;10:174.
62. Yu Y, Zhang Q, Sun K, Xiu Y, Wang X, Wang K, et al. Long non-coding RNA BBOX1 antisense RNA 1 increases the apoptosis of granulosa cells in premature ovarian failure by sponging miR-146b. Bioengineered 2022;13:6092-9.
63. Sun YT, Cai JH, Bao S. Overexpression of lncRNA HCP5 in human umbilical cord mesenchymal stem cell-derived exosomes promoted the proliferation and inhibited the apoptosis of ovarian granulosa cells via the musashi RNA-binding protein 2/oestrogen receptor alpha 1 axis. Endocr J 2022;69: 1117-29.
64. Wang S, Lin S, Zhu M, Li C, Chen S, Pu L, et al. Acupuncture reduces apoptosis of granulosa cells in rats with premature ovarian failure via restoring the PI3K/Akt signaling pathway. Int J Mol Sci 2019;20:6311.
65. Li N, Liu L. Mechanism of resveratrol in improving ovarian function in a rat model of premature ovarian insufficiency. J Obstet Gynaecol Res 2018;44:1431-8.
66. Yang Z, Du X, Wang C, Zhang J, Liu C, Li Y, et al. Therapeutic effects of human umbilical cord mesenchymal stem cell-derived microvesicles on premature ovarian insufficiency in mice. Stem Cell Res Ther 2019;10:250.
67. Vo KCT, Kawamura K. In vitro activation early follicles: from the basic science to the clinical perspectives. Int J Mol

Sci 2021;22:3785.
68. Laronda MM, Jakus AE, Whelan KA, Wertheim JA, Shah RN, Woodruff TK. Initiation of puberty in mice following decellularized ovary transplant. Biomaterials 2015;50:20-9.
69. Kniazeva E, Hardy AN, Boukaidi SA, Woodruff TK, Jeruss JS, Shea LD. Primordial follicle transplantation within designer biomaterial grafts produce live births in a mouse infertility model. Sci Rep 2015;5:17709.

Received: 28 July 2022. Accepted: 28 December 2022.

European Journal of Histochemistry 2023; 67:3506
doi:10.4081/ejh.2023.3506